Journal of Alloys and Compounds 509 (2011) 9934–9937

Contents lists available at ScienceDirect

Journal of Alloys and Compounds

journal homepage: www.elsevier.com/locate/jallcom

$Ba(Ti_{1-x}Sn_x)O_3$ ($x = 0.13$) nanomaterials produced by low-temperature aqueous synthesis

Marin Cernea [a,*], Roxana Trusca [b], Roxana Radu [a], Cristina Valsangiacom [a]

[a] National Institute of Materials Physics, P.O. Box MG-7, Bucharest-Magurele, 077125, Romania
[b] METAV-R&D S. A., P.O. 22, Bucharest, Romania

ARTICLE INFO

Article history:
Received 8 April 2010
Accepted 30 July 2011
Available online 22 August 2011

Keywords:
Powders-chemical preparation
Grain size
Dielectric properties
Ferroelectric properties
$BaTiO_3$ and titanates

ABSTRACT

$BaTi_{0.87}Sn_{0.13}O_3$ (BTS_{13}) nanopowder was prepared by low-temperature aqueous synthesis (LTAS) method. The evolution of the structure and microstructure of the precursor precipitate, heated at temperatures up to 1000 °C was studied by TGA, FT-IR, SEM and XRD techniques. The dried precipitate showed a microstructure consisting of nano-sized grains (~40 nm) with great tendency to agglomeration. $BaTi_{0.87}Sn_{0.13}O_3$ single phase was obtained at 800 °C. The ceramics prepared from as-obtained BTS_{13} powders (60–70 nm) show good dielectric and ferroelectric characteristics. The dielectric constant was about 4800 and the dielectric loss ($\tan\delta$) was 0.229 at 1 kHz and at the Curie temperature (31 °C). The remanent polarization (P_r) and the coercive field (E_C) of $Ba_{0.97}Ho_{0.03}TiO_3$ ceramics, at 1 kHz, were $P_r = 13\ \mu C/cm^2$ and $E_C = 0.89$ kV/cm. The ferroelectric parameters E_C and P_r decrease with increasing frequency in the domain 100 Hz to 10 kHz.

1. Introduction

$BaTiO_3$ doped with SnO_2, ($Ba(Ti_{1-x}Sn_x)O_3$; $x \leq 0.3$) exhibit ferroelectric properties and is used for capacitors and ceramic boundary layer capacitors [1–4]. In these ceramics, the isovalent Sn-substitution on the titanium (Ti) site reduces the temperature dependence and controls the room-temperature values of the dielectric characteristics [5–7], the relaxor behavior and its sensor applications [8].

Fine powders with uniform grain sizes are required to obtain dense ceramics with enhanced electrical properties [9]. As a result, chemical precipitation processes, alternative to the solid state reaction, have been developed. However, few reports on $Ba(Ti_{1-x}Sn_x)O_3$ synthesis by wet chemical methods as, hydrothermal method [2], synthesis from glycolate-precursor [9], precipitation method [10], and synthesis from precursor complexes [11] were published. Up to date, no work on preparation of $Ba(Ti_{1-x}Sn_x)O_3$ solid solution by low temperature aqueous solution method has been reported. Some papers regarding the synthesis of $BaSnO_3$ using LTAS method were published [12,13].

In this paper, precipitation of barium, titanium and tin precursors in strong alkaline solution and, characterization of the resulting powders and ceramics are presented.

2. Experimental procedure

The LTAS procedure requires relatively low temperature and can be carried out at atmospheric pressure, either in air or in an inert gas. BTS_{13} precursor precipitate was prepared by LTAS method starting from $TiCl_4$, $SnCl_4$ and $Ba(OH)_2$. Aqueous solutions of barium hydroxide $Ba(OH)_2$ (1 M), titanium (IV) chloride $TiCl_4$ (1.95 M) and tin (IV) chloride $SnCl_4$ (1.95 M) were prepared. All reagents (Merck) are of analytical grade purity. $TiCl_4$ and $SnCl_4$ mixture solution was slowly dropped into the solution of Ba^{2+}, while keeping it stirred, at 80 °C. In general, an increase of temperature produces a higher conversion rate and smaller particles. The molar ratio of $Ba(OH)_2$:$TiCl_4$:$SnCl_4$ used was 1:0.87:0.13 for $Ba(Ti_{1-x}Sn_x)O_3$, $x = 0.13$. A 1.5 molar stoichiometric excess of NaOH was added in order to neutralize HCl formed by $TiCl_4$ and $SnCl_4$ hydrolysis and to keep the batch at high pH value (pH = 13). At this pH, the solubility of $Ba(Ti,Sn)O_3$ is exceeded and appears the precipitate [14]. The method is based on the following reaction:

$$Ba(OH)_2 + 0.87TiCl_4 + 0.13SnCl_4 + 4NaOH = BaTi_{0.87}Sn_{0.13}O_3 + 4NaCl + 3H_2O$$

The synthesis was carried out in argon, under atmospheric pressure. After 2 h, the suspension was cooled down and washed with distilled water by decantation until the Na^+ and Cl^- ions were removed and the neutrality of the system was reached. The precipitate was dried at 100 °C and then heated up to 800 °C to obtain Ba (Ti,Sn)TiO_3 single phase. The ceramic samples were prepared by uniaxial pressing method at 200 MPa. The pellets with 12 mm diameter and 1.5 mm thick were sinterized at 1300 °C, for 2 h in air. Samples with apparent densities of 92% from theoretical density were obtained. The density of the pellets was measured by Archimedes's method (in water) using a density balance.

The thermogravimetric analysis was performed with SETARAM Setsys Evolution 18 in TG-DSC mod Thermal Analyzer. The sample was measured in an open cylindrical alumina crucible and the experiment conducted in synthetic air (80%N_2:20%O_2) at a flow rate of 16 ml/min. The temperature was calibrated with bismuth, aluminum and silver; temperature range of the experiments was between 275 and 1000 °C, and the heating rate was 10 °C/min. The enthalpies for endothermic and exothermic peaks were calculated with the CALISTO software.

* Corresponding author. Tel.: +40 21 369 0170/130; fax: +40 21 369 0177.
E-mail address: mcernea@infim.ro (M. Cernea).

0925-8388/$ – see front matter © 2011 Elsevier B.V. All rights reserved.
doi:10.1016/j.jallcom.2011.07.101

A mixture of the precipitate powder and KBr powder was used for infrared spectroscopy studies. FT-IR spectra were recorded using a Shimadzu FTIR spectrometer. Particle microstructures were investigated using a Hitachi S2600N scanning electron microscope.

The identification of the phases formed during calcinations was carried out using XRD analysis, in the range 20–80° (2θ), in a Bruker-AXS tip D8 ADVANCE diffractometer. For powder diffraction, CuKα1 radiation, (wavelength 1.5406 Å), a LiF crystal monochromator and Bragg–Brentano diffraction geometry were used.

The microstructure of the samples was investigated using a FEI Quanta Inspect F scanning electron microscope.

The temperature dependence of dielectric constant and dielectric losses were evaluated in the temperature range from −20 to 160 °C at 1 kHz, 10 kHz and 100 kHz using an Agilent 4263B LCR meter equipped with a thermostat. The electrical measurements were carried out in the metal–ferroelectric–metal (MFM) configuration where, M is silver and F is the ferroelectric sample ($BaTi_{0.87}Sn_{0.13}O_3$).

P–E loops were measured using aixACCT System with a modular designed electrical characterization system: the TF Analyzer 2000HS series. The dependence of the polarization *P* on an alternating electric field *E* with 5 kV/mm amplitude was measured at frequencies of 1 kHz and 10 kHz, with the aid of a Sawyer–Tower circuit. A triangular waveform was chosen for the electric field cycle.

3. Results and discussion

3.1. Thermal analyses

Thermal behavior of the $Ba(Ti,Sn)O_3$ precipitate precursor from 275 to 1000 °C is presented in Fig. 1.

The removal of the moisture takes place from the room temperature to 378 °C. An endothermic peak of 50.2 J/g, centered at 345 °C, is associated to this process. The second endothermic reaction 5.7 J/g, take place from 445 and 500 °C and can be ascribed to the decomposition of barium carbonate also observed by XRD. $BaCO_3$ is always present in the powders prepared in alkaline conditions due to the partial carbonatation of barium hydroxide with CO_2 from the atmosphere. The exothermic effect of 4.3 J/g, observed at 780 °C, corresponds to the forming reaction of $Ba(Ti, Sn)TiO_3$ solid solution. A continually weight loss up to 900 °C can be related to the elimination of OH groups, as observed by IR spectroscopy. The OH groups are present in the crystal lattice [15] and at the grains surface [16].

3.2. Infrared spectroscopy

The Fourier transform infrared spectroscopy (FT-IR) spectrum of the $BaTi_{0.87}Sn_{0.13}O_3$ (BTS_{13}) precipitate was recorded on the dried precipitate at 100 °C. As shown in Fig. 2, the sample presented IR absorption bands at 3600–3200, 1445, 858, 693 and 550 cm^{-1}.

The dried precipitate presents a large band at 3400 cm^{-1} attributed to adsorbed water molecules [17,18]. The bands at 1445, 858 and 693 cm^{-1} correspond to $BaCO_3$ which is always present

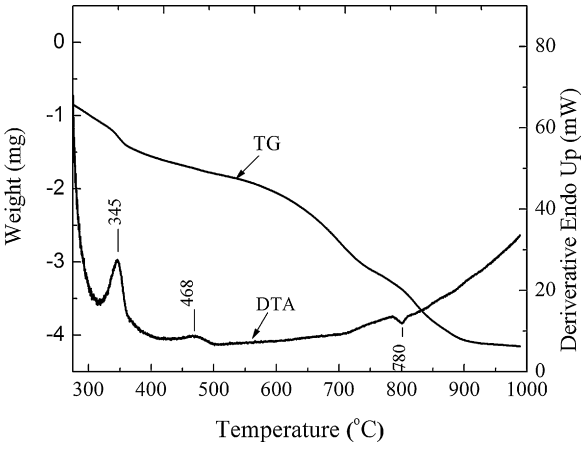

Fig. 1. Thermal analyses of the $BaTi_{1-x}Sn_xO_3$, $x = 0.13$ precipitate precursor.

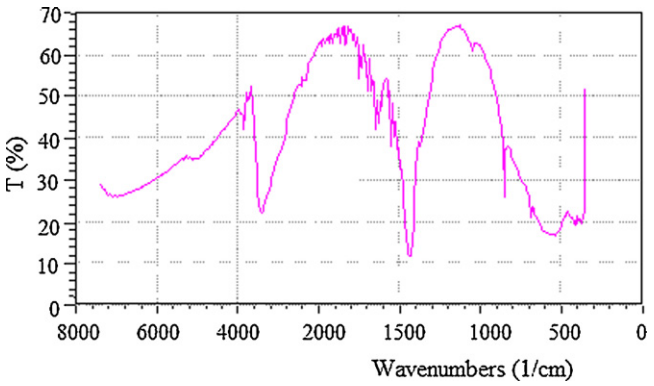

Fig. 2. FTIR spectrum of $BaTi_{0.87}Sn_{0.13}O_3$ precipitate dried at 100 °C.

when barium hydroxide is used. The bands below 900 cm^{-1}, are due to metal-oxygen bonds [19,20]. The band characteristic to the octahedron O_6 vibration, located at 550 cm^{-1}, is approximative symmetrical and suggests the cubic structure of the grains.

3.3. SEM analysis

The SEM micrograph of Ba, Ti and Sn oxalate precipitate dried at 100 °C (Fig. 3a), shows a microstructure consisting of very fine grains of about ~40 nm in diameter.

The precipitate heated at 800 °C presents homogenous sized particles of about 60–70 nm (Fig. 3b). However, the powders present a rather strong degree of agglomeration due to the interactions of OH^- groups present on the grains surface. Fig. 3c shows the surface microstructure of $BaTi_{0.87}Sn_{0.13}O_3$ pellets, sintered at 1300 °C, 2 h in air. To obtain the SEM micrograph of sintered ceramic, the surface of $BaTi_{0.87}Sn_{0.13}O_3$ pellet was coated with a thin layer of gold. The ceramics have a dense structure with submicronic grains. There is a distribution in which small grains of ~100 nm coexist with grains of 200–300 nm.

3.4. XRD analysis

Fig. 4 shows the X-ray diffraction patterns of BTS_{13} precursor fired at 100 °C and 800 °C and also, of pellets sintered at 1300 °C, 2 h in air. The XRD diagram of the precipitate heated at 100 °C, showed all the peaks of $BaCO_3$ orthorhombic phase [21] and very small peaks of $BaTiO_3$ cubic phase.

The precipitate powder heated at 800 °C, 2 h in air, presented a single phase with the perovskite structure of cubic $BaTiO_3$ (Fig. 4) [22]. The result is similar to the previous work [5]. The cubic $BaTiO_3$ phase can be correlated with the very fine grained BTS_{13} powder (40–70 nm).

3.5. Dielectric properties

Fig. 5 shows the dependence of the relative dielectric constant (a) and dielectric loss (b) versus temperature and frequency for BTS_{13} sintered ceramic.

The pellets show permittivity peaks corresponding to their ferroelectric to paraelectric phase transition. Dielectric peaks are observed in the temperature range of −20 to 160 °C, and it is noted that the maximum of the dielectric constant (ε_m) reaches reasonably high values in $BaTi_{1-x}Sn_xO_3$ solid solution, $\varepsilon_m = 4800$ at 1 kHz and $T_m = 31$ °C, $\varepsilon_m = 4850$ at 10 kHz and $T_m = 32$ °C and, $\varepsilon_m = 4780$ at 100 kHz and $T_m = 33$ °C. With increasing frequency, the temperature with the maximum dielectric constant (T_m) increases (Table 1). The frequency dependence of dielectric constant indicates that the higher dielectric constant was obtained for frequency of 10 kHz.

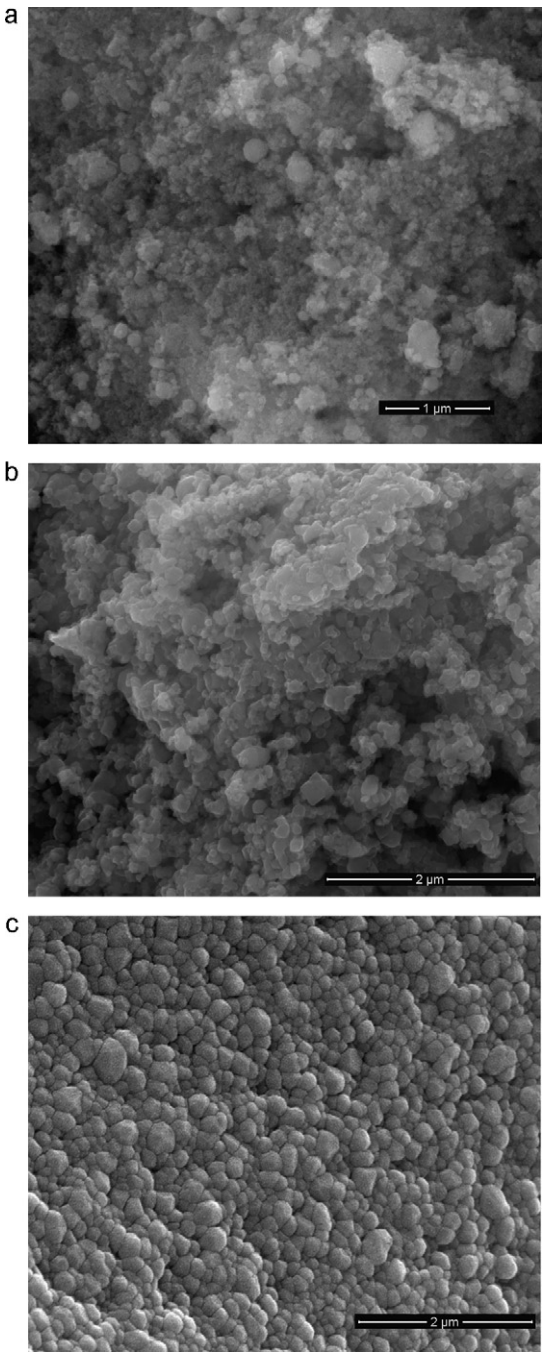

Fig. 3. SEM photomicrographs of the $BaTi_{1-x}Sn_xO_3$, $x = 0.13$ powder heated at 100 °C (a) and 800 °C (b), and sintered ceramic (c).

Dielectric losses tangent (δ) of $Ba(Ti_{0.87}Sn_{0.13})O_3$ ceramics were 0.167 at 100 kHz, 0.234 at 10 kHz and, 0.229 at 1 kHz, at the Curie temperatures (Fig. 5). These results indicated good dielectric characteristics of BTS_{13} which are comparable with the literature data [16,19].

The dielectric curves of $Ba(Ti_{0.87}Sn_{0.13})O_3$ ceramic show notable diffused phase transition behaviors (DPT). Martirena [23] and Uchino [24] proposed the following empirical relation for the temperature variation of ε, for DPT:

$$\frac{1}{\varepsilon} = \frac{1}{\varepsilon_m} + \frac{(T - T_m)^\gamma}{C'} \quad (1)$$

where γ is the critical exponent and C' is the Curie–Weiss-like constant. It is believed that the power factor γ close to 1 suggests normal ferroelectrics, while close to 2 suggests relaxor ferroelectrics. The experimental dielectric constant data was fitted to Eq. (1) very well and the obtained γ values are shown in Table 1.

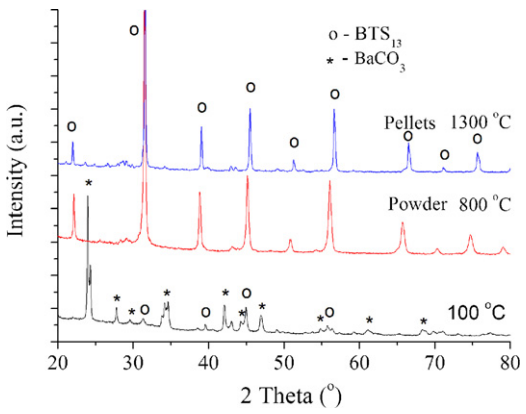

Fig. 4. X-ray diffraction patterns of the $BaTi_{1-x}Sn_xO_3$, $x = 0.13$, powders heated at 100 °C and 800 °C, and, sintered pellets.

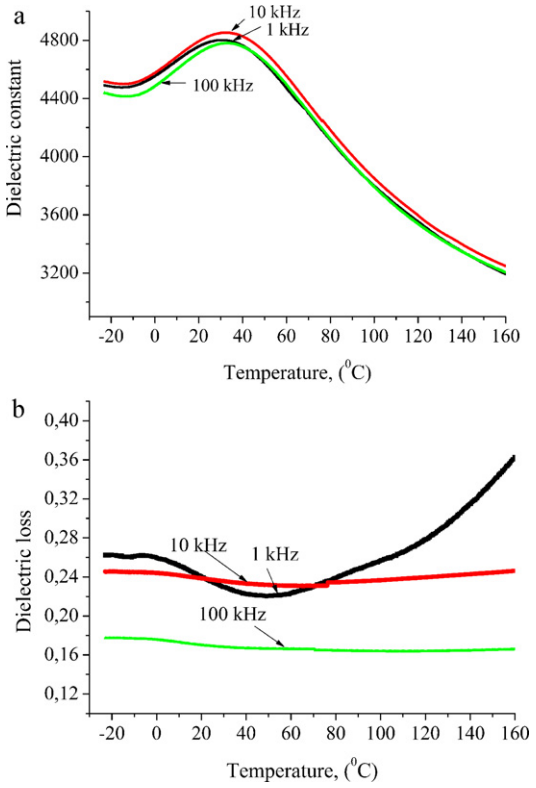

Fig. 5. Temperature and frequency dependence of (a) dielectric constant and (b) loss tangent (δ) of $BTS_{0.13}$ ceramics.

The results suggest that BTS solid solution within the investigated frequency range exhibits reasonable relaxor behaviors and the relaxor tendency grows with increasing frequency, which also are proved by the *P–E* behavior.

Table 1
Curve fitting results for $Ba(Ti_{0.87}Sn_{0.13})O_3$ ceramic, at various frequencies.

Frequency, (kHz)	T_m, (°C)	ε_m	γ
1	31	4800	1.536
10	32	4850	1.597
100	33	4780	1.622

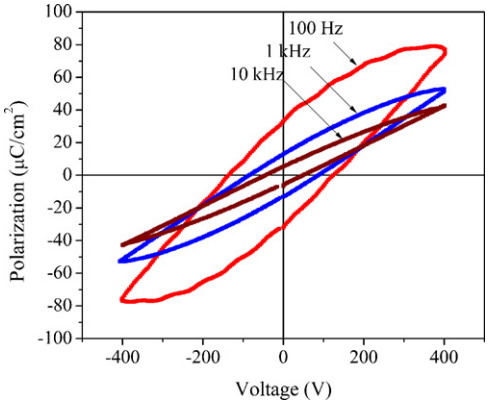

Fig. 6. *P–E* dynamic hysteresis loops measured at 100 Hz to 10 kHz for BTS_{13} ceramic.

Fig. 6 gives polarization–electric field (*P–E*) data determined at various frequencies for BTS_{13} ceramic, sintered at 1300 °C, in air.

The polarization hysteresis loops were obtained for $Ba(Ti_{0.87}Sn_{0.13})O_3$ solid solution at various frequencies and at room temperature, and gradually became smaller and weaker with increasing frequency. The aim of the measurement is to highlight the ferroelectricity through the *P–E* hysteresis loop. Dynamic hysteresis implies continuous integration of the current that goes through a ferroelectric capacitor during a complete variation cycle of the AC voltage.

As it can be seen from the data plotted in Fig. 6, the ferroelectric hysteresis loops of BTS_{13} do not show a true saturation branch. The samples exhibit very small hysteresis with almost linear dependence of *P–E*. Several possible causes result in a strong suppression of macroscopic ferroelectric character and, consequently, in the observed slim and nearly linear *P–E* loop [25], with increasing frequency. Both parameters E_C and P_r decrease with the increase of frequency. The P_r was 34 μC/cm² at 100 Hz, 13 μC/cm² at 1 kHz, and 5.3 μC/cm² at 10 kHz, while the E_C was 1.24 kV/cm at 100 Hz, 0.89 kV/cm at 1 kHz, and 0.41 kV/cm at 10 kHz. These results are in good agreement with literature data [26]. Frey et al. [27], and Takeuchi et al. [28] had reported progressive lowering of remanent polarization and hysteresis with decreasing grain size.

4. Conclusions

Sn-doped $BaTiO_3$ precursor precipitate has been prepared by LTAS method at 80 °C, in strong alkaline solution. The thermal analyses and X-ray diffraction indicated that Ba(Ti, Sn)TiO_3 solid solution is obtained, as single phase with the perovskite structure of cubic $BaTiO_3$, by heating the precipitate at 800 °C. BTS_{13} powder obtained at 800 °C presents homogenous sized particles of about 60–70 nm. The ceramics obtained from this powder shown dense structure with submicronic grains (100–300 nm). At the Curie temperatures (31–33 °C) the dielectric constants were between 4800 and 4780 while the dielectric losses (tanδ) were in the range 0.229–0.167 at frequencies of 1–100 kHz interval. The dielectric curves of $Ba(Ti_{0.87}Sn_{0.13})O_3$ ceramic, at various frequencies, shown diffused phase transition behaviors. The ferroelectric parameters E_C and P_r decrease with the increase of frequency in the domain 100 Hz to 10 kHz. These dielectric and ferroelectric properties of BTS_{13} prove that the LTAS method is able to prepare nanopowders and ceramics with applications in electronics field.

References

[1] E.C. Subbarao, Ferroelectrics 35 (1981) 143–148.
[2] R. Vivekanandan, T.R.N. Kutty, Ceram. Int. 14 (1988) 207–216.
[3] R. Wernicke, Ber. Dtsch. Keram. Ges. 55 (1978) 356–358.
[4] H. Brauer, Z. Angew. Phys. 29 (1970) 282–287.
[5] G.A. Smolensky, J. Phys. Soc. Jpn. 28 (1970) 26–37.
[6] N. Yasuda, H. Ohwa, S. Asano, Jpn. J. Appl. Phys. 35 (1996) 5099–5103.
[7] K. Oh, K. Uchino, L.E. Cross, J. Am. Ceram. Soc. 77 (1994) 2809–2816.
[8] S.G. Lu, Z.K. Xu, H. Chen, Appl. Phys. Lett. 85 (2004) 5319–5321.
[9] L. Geske, V. Lorenz, T. Muller, L. Jager, H. Beige, H.-P. Abicht, V. Müller, J. Eur. Ceram. Soc. 25 (2005) 2537–2542.
[10] M. Cernea, D. Piazza, A. Manea, E. Vasile, C. Galassi, J. Am. Ceram. Soc. 90 (2007) 1728–1732.
[11] R. Koferstein, L. Jager, V. Lorenz, H.P. Abicht, J. Woltersdorf, E. Pippel, H. Gorls, Solid State Sci. 7 (2005) 1280–1288.
[12] P. Nanni, M. Leoni, V. Buscaglia, G. Aliprandi, J. Eur. Ceram. Soc. 14 (1994) 85–90.
[13] M. Leoni, M. Viviani, P. Nanni, V. Buscaglia, J. Mater. Sci. Lett. 15 (1996) 1302–1304.
[14] M. Klee, J. Mater. Sci. Lett. 8 (1989) 985–988.
[15] G. Busca, V. Buscaglia, M. Leoni, P. Nanni, Chem. Mater. 6 (1994) 955–961.
[16] D. Hennings, S. Schreinemacher, J. Eur. Ceram. Soc. 9 (1992) 41–46.
[17] M. Stockenhuber, H. Mayer, J.A. Lercher, J. Am. Ceram. Soc. 76 (1993) 1185–1190.
[18] W. Li, J. Li, J. Guo, J. Eur. Ceram. Soc. 23 (2003) 2289–2295.
[19] P.K. Dutta, P.K. Gallagher, J. Twu, Chem. Mater. 5 (1993) 1739–1743.
[20] G. Pfaff, V.D. Hildenbrand, H. Fuess, J. Mater. Sci. 17 (1998) 1983–1985.
[21] M.Y. Colby, J.B. LaCoste, Z. Kristallogr, Kristallgeom. Kristallphys. Kristallchem. 90 (1935) 1.
[22] R.H. Buttner, E.N. Maslen, Acta Crystallogr. Sect. B: Struct. Sci. 48 (1992) 764–769.
[23] H.T. Martirena, J.C. Burfoot, Ferroelectrics 7 (1974) 151–152.
[24] K. Uchino, S. Nomura, Ferroelectr. Lett. Sect. 44 (1982) 55–61.
[25] X. Deng, X. Wang, H. Wen, L. Chen, L. Li, Appl. Phys. Lett. 88 (2006) 252905–252908.
[26] T. Wang, X.M. Chen, X.H. Zheng, J. Electroceram. 11 (2003) 173–178.
[27] M.H. Frey, Z. Xu, P. Han, D.A. Payne, Ferroelectrics 206-207 (1998) 337–353.
[28] T. Takeuchi, C. Capiglia, N. Balakrishnan, Y. Takeda, H. Kageyama, J. Mater. Res. 17 (2002) 575–581.